Çukurova Üniversitesi Mühendislik Mimarlık Fakültesi Dergisi, 33(1), ss. 143-150, Mart 2018
*Çukurova University Journal of the Faculty of Engineering and Architecture, 33(1), pp. 143-150, March 2018*

# Effect of Eu Doping on the Structural, Magnetic and Magnetocaloric Properties in $La_{0.85}Ag_{0.15}MnO_3$

**Mustafa AKYOL**[*1]

[1]*Adana Bilim ve Teknoloji Üniversitesi, Mühendislik Fakültesi, Malzeme Mühendisliği Bölümü, Adana*

*Geliş tarihi: 05.12.2017* *Kabul tarihi: 14.03.2017*

## Abstract

In this research, the effect of Eu doping on the structural, magnetic and magnetocaloric properties in $La_{0.85}Ag_{0.15}MnO_3$ sample synthesized by sol-gel technique has been studied. The structural analysis show that crystal structure of the sample is found as rhombohedral being the same as undoped sample. But, the average particle size decreases when Eu is doped in the main structure. In the magnetic analysis, a magnetic transition is observed from ferromagnetic to paramagnetic phase around 192 K. The maximum magnetic entropy change $(-\Delta S_M)_{\max}$ and relative cooling power (RCP) values were found as 2.78 J/kgK and 142.31 J/kg under 5 T field change.

**Keywords:** Sol-gel, Eu-doping, Curie temperature, Magnetic entropy change, Magnetocaloric effect

## $La_{0.85}Ag_{0.15}MnO_3$ Yapısına Eu Katkılamasının Yapısal, Manyetik ve Manyetokalorik Özelliklere Etkisi

## Öz

Bu araştırmada, sol-jel tekniği ile sentezlenen $La_{0.85}Ag_{0.15}MnO_3$ numunesine Eu katkılamasının yapısal, manyetik ve manyetokalorik özelliklere etkisi çalışılmıştır. Yapısal analizler, örneğin; kristal yapısının katkısı örnek ile aynı olan rombohedral yapıda olduğunu göstermiştir. Fakat ortalama parçacık boyutu, Eu katkılaması gerçekleştirildiğinde ana yapıya göre azalmaktadır. Yaklaşık 192 K'de feromanyetik-paramanyetik faz geçişinin olduğu manyetik analizlerden gözlenmiştir. Maksimum manyetik entropi değişimi $(-\Delta S_M)_{max}$ ve göreceli soğutma gücü (RCP) değerleri 5 T alan değişimi altında sırasıyla 2,78 J/kgK ve 142,31 J/kg olarak bulunmuştur.

**Anahtar Kelimeler:** Sol-jel, Eu-katkılama, Curie sıcaklığı, Manyetik entropi değişimi, Magnetokalorik etki

[*]Sorumlu yazar *(Corresponding author)*: Mustafa AKYOL, *makyol@adanabtu.edu.tr*

## 1. INTRODUCTION

Next generation cooling systems would be magnetically cooling (MC) ones like the commonly used vapor compression technology due to its low energy dissipations and being environmental friendly [1-3]. The main physical phenomenon of magnetic cooling system is known as magnetocaloric effect (MCE) defined as magnetic entropy change when external magnetic field is applied to the magnetocaloric material.

Although MCE has been studied by various magnetic material groups [2], perovskite manganites chemical formula $RE_{1-x}C_xMnO_3$ (RE: Rare-Earth cation-A site, C: Alkali-metal or Alkaline- earth cation- B cite) have been searched for extensively because of their advantages for practical applications, such as exhibiting large spontaneous magnetization value and its abrupt drop at phase transition temperature, high chemical stability, much smaller thermal and field hysteresis than any rare earth and 3*d*- transition metal based alloys and being cheapest material among existing magnetic refrigerants [4-8].

Since A-site ions play a crucial role in the physical properties of manganites, the research on the 3*d* and/or 4*f* elements substitution/adding into the A-site attracts great attention. So far, divalent alkaline earth elements doped manganites have been extensively examined to understand their magnetocaloric and physical properties [2,9-11]. However, monovalent elements doped manganites and/or the effect of changing trivalent elements with La ions have become relatively new works in the magnetocaloric community [1,11-15]. In monovalent element doped manganites, researchers pay attention to the structure of $La_{1-x}Ag_xMnO_3$ series due to their large MCE values and convenient $T_C$ values for practical applications [16,17]. Moreover, because of the absence of Eu-doped $La_{0.85}Ag_{0.15}MnO_3$ structure in the literature, the effect of Eu-doping into the $La_{0.85}Ag_{0.15}MnO_3$ perovskite sample on the structural and magnetocaloric properties has been worked comprehensively.

## 2. EXPERIMENTAL PROCESS

Polycrystalline Eu-doped $La_{0.85}Ag_{0.15}MnO_3$ sample was synthesized by sol-gel method using high purity powders of $La_2O_3$, $Mn(NO_3)_2{\cdot}4H_2O$, $AgNO_3$ and $Eu_2O_3$ as starting materials. Monoethylene glycol (99.9% purity), citric acid monohydrate (99.9% purity) and nitric acid (70% purity) were used as a chelating substance. Obtained material was mixed and heated by a magnetic stirrer at 300ºC until obtaining gel-like precipitation. This precursor was heated at 500ºC for 1 h to burn. The final material was ground by using an agate mortar to obtain fine powders. Afterwards, the material was pressed into pellet form and sintered at 970ºC for 24 h in air. The sample is labeled as Eu:LAM through the manuscript.

Crystal structure of the sample was determined by X-ray diffraction (XRD) technique using Cu-Kα radiation. The XRD pattern was analyzed by the MATCH! 2 software based on the Rietveld method and X Pert High score Plus. Morphology of the sample was studied by Scanning Electron Microscope (SEM). Magnetization measurements were carried out using a vibrating sample magnetometer (Quantum Design PPMS-DyneCool). The magnetic entropy change, $\Delta S_M$ values were obtained from isothermal magnetization measurements near the phase transition region.

## 3. RESULTS AND DISCUSSIONS

The structure of the powdered sample is characterized by XRD. Rietveld refinement for the sample has been done by using Match software. The XRD patterns of the compound given in Fig. 1 indicate the polycrystalline behavior. The characteristic diffraction peaks of the sample are indexed as the rhombohedral structure with $R\bar{3}c$ space group. In addition to the characteristic peaks of the perovskite structures, small reflections indexed as $EuMn_2O_5$ with *Pbam* space group is observed. Due to the non-ferromagnetic nature of the $REMn_2O_5$ structure [18], impurity phase doesn't affect the magnetocaloric behavior of the sample. To compare the structural parameters, the

lattice parameters and unit cell volume for LAM [14], Eu:LAM and Gd:LAM [15] samples have been tabulated in Table 1, where lattice parameters decrease by changing Eu with Gd, as well as just adding Eu into the lattice. This situation arises from the smaller ionic radius of Gd than Eu [19]. Substitution of an element with smaller ionic radius one yields to decrease average A site ionic radius, $r_A$ [14], decreasing $r_A$ yields to increase mismatch effect $\sigma^2$ [14]. Decreasing $r_A$ and increasing $\sigma^2$ yields to tilting of $MnO_6$ octahedra.

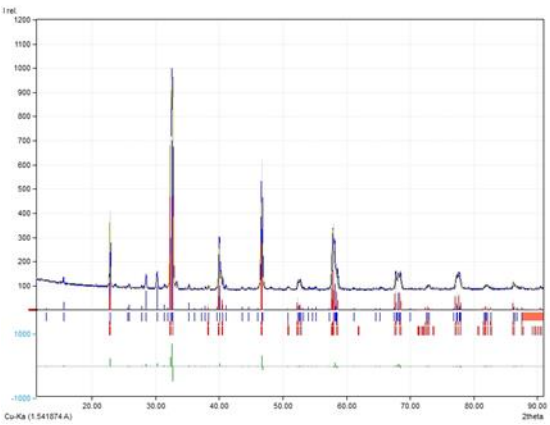

**Figure 1.** XRD patterns of Eu:LAM sample

**Table 1.** Unit cell parameters and unit volume for LAM, Eu:LAM and Gd:LAM samples

| Sample | a=b (Å) | c (Å) | V (Å$^3$) |
|---|---|---|---|
| **LAM [14]** | 5.522(3) | 13.373(4) | 353.24(1) |
| **Eu:LAM** | 5.511(1) | 13.371(4) | 351.67(1) |
| **Gd:LAM [15]** | 5.509(1) | 13.369(3) | 351.46(1) |

The morphology and element analysis have been characterized by scanning electron microscope (SEM) images and energy-dispersive X-ray (EDS) spectrums, respectively. Figure 2a indicates the SEM image of the Eu-doped LAM sample. The grains are settled closely packed and their distribution is homogeneous confirmed by plotting grain size distribution taking 100 randomly selected grains in the structure (see Fig.2b). The average grain size is found as 0.72 μm which is much smaller than LAM sample (1.23 μm) [14]. In the EDX spectrum, we have observed all the expected element peaks without impurity (see inset of Fig.2a), which means no loss of any integrated elements, and no impurity element during the sintering process occurred. The desired chemical compounds of the sample $(La_{0.9}Eu_{0.1})_{0.85}Ag_{0.15}MnO_3$) is confirmed with the EDX by measuring at various points in the SEM images.

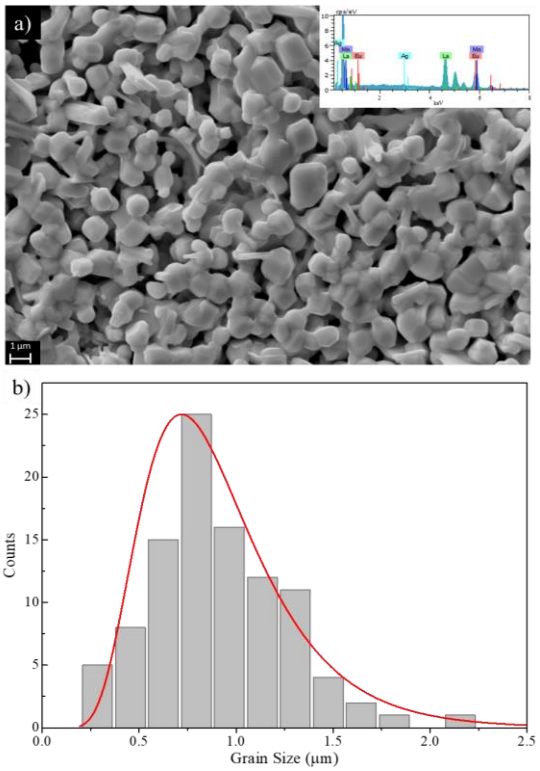


**Figure 2.** a) SEM image of Eu:LAM sample and b) its grain size distribution

Magnetic properties of the Eu:LAM sample have been investigated by temperature (*M-T*) and magnetic field (*M-H*) dependence magnetization measurements. First, we have performed *M-T* measurement in a three cycles called as zero-field cooled (ZFC), field-cooled (FC) and field-heated (FH) process. Figure 3 inhibits the *M-T* curves that magnetizations for all cycles increase suddenly with decreasing temperature. This increase in magnetization is coming from the critical magnetic transition point where the magnetic coupling changes from paramagnetic to ferromagnetic. This critical point of the temperature is called Curie temperature ($T_C$) determined from the inverse

susceptibility versus temperature curves depicted in inset of Fig.3a. The $T_C$ is found as 192 K for Eu:LAM sample. Although the concentration of Eu is only 10% compared to La in the main lattice, the critical temperature decreases from 262 K to 192 K by the substitution of $Eu^{3+}$ for $La^{3+}$ [14]. The reason of decreasing in $T_C$ can be explained that the decreasing $<r_A>$ and $t_f$ values yield to decrease of the local stress in $MnO_6$ octahedron, causing the increasing rotation in $MnO_6$ octahedron [20,21]. This increase in rotation yields to weakening of double exchange interaction by localizing of $e_g$ electrons and hence $T_C$ value of the compounds decreases. Moreover, the increasing of $\sigma^2$ induces a lattice strain by causing a random displacement of oxygen ions, thereby resulting in a distortion of the $MnO_6$ octahedra, and hence the $e_g$ electrons are localized. So, these changes lead to decrease of $T_C$ value of the compounds by weakening double exchange interaction.

The effective magnetic moment of sample can also be found from the inverse susceptibility, $1/\chi$, versus $T$ curve (inset of Fig. 3a). A typical Curie-Weiss behavior is observed above the $T_C$ where $1/\chi$ changes almost linearly with the temperature that can be fitted by $\chi = C/(T - \theta)$, where $C$ is the Curie constant and $\theta$ is the paramagnetic Curie-Weiss temperature. Above $T_C$, the extrapolation of the straight lines cut the temperature axis at Curie-Weiss temperature which is an indication of the nature and strength of magnetic coupling in the structure. Then, the effective magnetic moment, $\mu_{eff}$ was derived by using $\mu_{eff}^2 = 3k_BC/N^2\mu_B^2$ where $N$ is the Avogadro's number, $\mu_B$ is the Bohr magneton, $k_B$ is the Boltzmann constant, and $C$ is obtained from the slopes of the straight lines mentioned above. The $\mu_{eff}$ value is found as $2.99\mu_B$ which is smaller than the LAM sample [14]. Magnetic hysteresis measurement has been carried out at 5 K to determine the coercive field ($H_c$), saturation ($M_s$) and remanence magnetization ($M_r$) (see Fig.3b). The $M$-$H$ curve presents that the magnetization increases suddenly with applied magnetic field and it saturates (~72 emu/g) under low magnetic field (~600 Oe). But, the sample has no measurable coercive field and remanence magnetization.

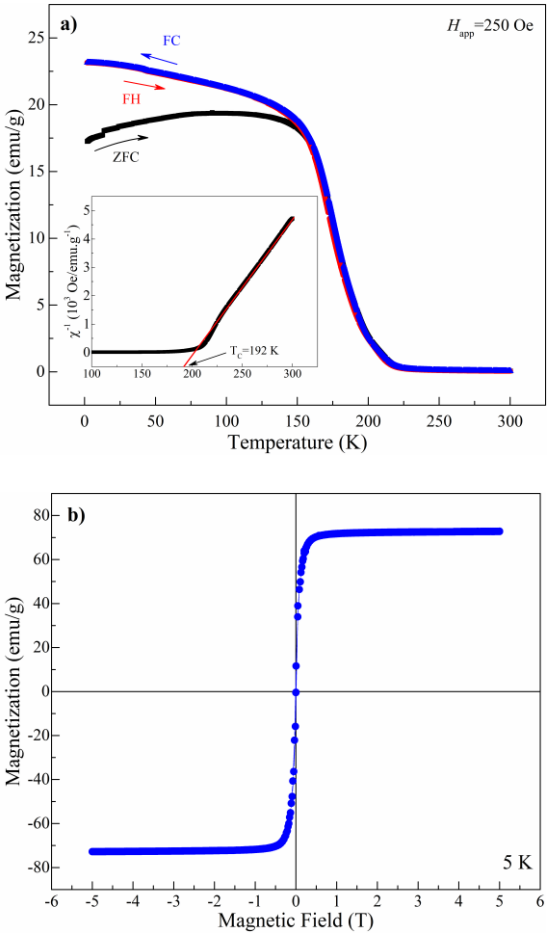


**Figure 3.** a) Temperature dependence magnetization of Eu:LAM sample. Inset: Inverse susceptibility as a function of temperature, b) Magnetic hysteresis of Eu:LAM sample at 5 K temperature

According to the classical thermodynamic theory, the magnetic entropy change, $\Delta S_M$ generated by the changing of a magnetic field from 0 to $H_{max}$ can be expressed as following [3,22,23];

$$\Delta S_M(T,H) = S_M(T,H) - S_M(T,0) = \int_0^{H_{max}} \left(\frac{dM}{dT}\right)_H dH \qquad (1)$$

where $H_{max}$ is the maximum applied magnetic field. According to Eq. 1, the magnetic entropy change can be found by measuring isothermal magnetization around the Curie temperature.

Therefore, we performed magnetization measurements by taking initial *M-H* curves from 139 to 232 K by 3 K steps exhibited in Fig.4. In the FM region ($T < T_C$), the *M(H)* curves are nonlinear behavior, as expected. They become linear when the measurement temperature is higher than the critical temperature ($T > T_C$) where the magnetic phase is paramagnetic.

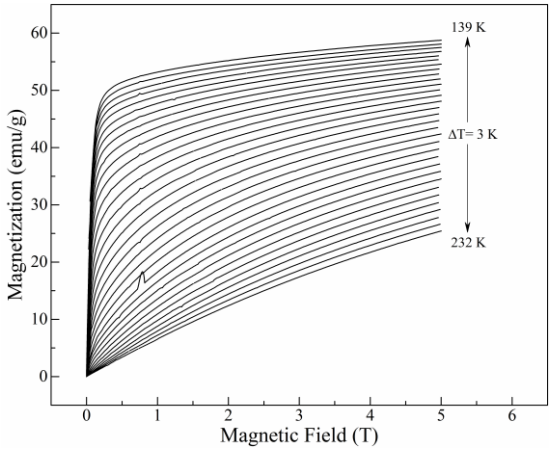


**Figure 4.** Isothermal magnetization curves of Eu:LAM sample measured around Curie temperature with a 3 K step

The magnetic entropy changes as a function of temperature were determined from the magnetization isotherms using Eq. 1. Figure 5 shows $-\Delta S_M$ as a function of temperature under 1, 3 and 5 T external magnetic fields. It can be seen that the maximum values of $\Delta S_M$ are located at temperature very close to the magnetic transition temperature. But, we observed a slight shift in the temperature of the maximum $\Delta S_M$ to higher temperature when applied field is increased. This might be related to the magnetic inhomogeneity, and short-range magnetic order regions [24,25]. The maximum $\Delta S_M$ values of the Eu:LAM sample is calculated as 0.83, 2.08 and 2.78 J/kgK under 1,3 and 5 T magnetic field, respectively. Although these values are lower than the LAM [14] sample, they are comparable to typical manganites [2]. The reason in the reduction of magnetic entropy change can be explained by the fact that the surface atomic layer of magnetic nanoparticles is generally characterized to be magnetically disordered layer (or magnetically dead layer) and has no contribution to the magnetization. It is well known that when the size of particle is decreased, the nonmagnetic surface layer is expected to become remarkable. Thus, this leads to a decrease in the magnetization. In the Eu:LAM sample, the average particle size is lower than LAM sample indicating that Eu doping increases surface atomic layer and reduces the strength of double exchange interaction [20, 21]. In addition, the lowering particle size reduces both $T_C$ and $\Delta S_M$ value of sample.

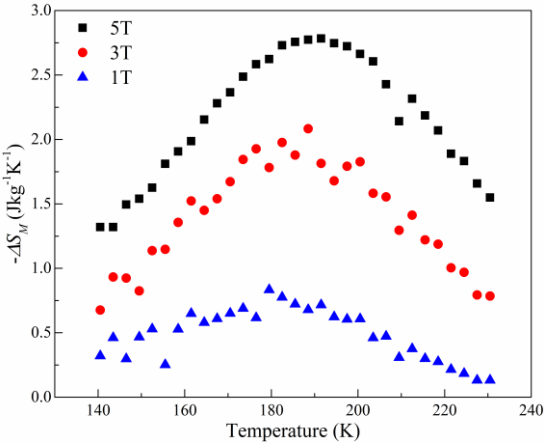


**Figure 5.** The temperature dependence of $\Delta S_M$ for Eu:LAM sample at different magnetic fields

Further magnetocaloric properties of the sample have been investigated by the calculation of relative cooling power (RCP), which is an important property of magnetic refrigerant in terms of the cooling efficiency and ascertained. RCP values can be found the relation of RCP = $-\Delta S_M^{max} \times \delta T_{FWHM}$ [2] where $\delta T_{FWHM}$ is full width at half maximum of $\Delta S_M$. The RCP values are found as 45.92, 101.75 and 142.31 J/kg under 1, 3 and 5 T magnetic fields, respectively.

## 4. CONCLUSIONS

The effects of Eu-doping into the $La_{0.85}Ag_{0.15}MnO_3$ perovskite manganite synthesized by sol-gel technique on the structural, magnetic and magnetocaloric properties have been studied. The

crystal structure of Eu:LAM sample is found as same as LAM that is rhombohedral. In addition, we observed that the average particle size determined from the SEM images decreases by adding Eu into the lattice. The temperature dependence magnetization measurements show that the sample has ferromagnetic to paramagnetic phase transition at around 192 K temperature. The isothermal magnetization measurements near the phase transition region has been performed to determine the magnetic entropy change. The maximum magnetic entropy change and relative cooling power were determined as 0.83, 2.08 and 2.78 J/kgK and 45.92, 101.75 and 142.31 J/kg under an applied field change of 1.0, 3.0 and 5 T, respectively. It is found that the relatively large $\Delta S_M$ and RCP values around $T_C$ which are comparable to typical magnetocaloric based manganites and they show applicability, as a potential magnetic refrigerant.

## 5. ACKNOWLEDGEMENT

I would like to thank to Dr. Ahmet Ekicibil and Dr. Ali Osman Ayaş for their valuable discussion.

## 6. REFERENCES

**1.** Atalay, S., Kolat, V.S., Gencer, H., Adiguzel, H.I., 2006. Magnetic Entropy-change in $La_{0.67-x}Bi_xCa_{0.33}MnO_3$ Compound. Journal of Magnetism and Magnetic Materials, 305 (2), 452-456.

**2.** Phan, M.H., Yu, S.C., 2007. Review of the Magnetocaloric Effect in Manganite Materials. Journal of Magnetism and Magnetic Materials, 308 (2), 325-340.

**3.** Sande, P., Hueso, L.E., Miguéns, D.R., Rivas, J., Rivadulla, F., López-Quintela, M.A., 2001. Large Magnetocaloric Effect in Manganites with Charge Order. Applied Phycis Letters, 79 (13), 2040-2042.

**4.** Chau, N., Nhat, H.N., Luong, N.H., Minh, D.L., Tho, N.D., Chau, N.N., 2003. Structure, Magnetic, Magnetocaloric and Magnetoresistance Properties of $La_{1-x}Pb_xMnO_3$ Perovskite. Physica B: Condensed Matter, 327 (2), 270-278.

**5.** Kolat, V.S., Izgi, T., Kaya, A.O., Bayri, N., Gencer, H., Atalay, S., 2010. Metamagnetic Transition and Magnetocaloric Effect in Charge-ordered $Pr_{0.68}Ca_{0.32-x}Sr_xMnO_3$ (x=0, 0.1, 0.18, 0.26 and 0.32) compounds. Journal of Magnetism and Magnetic Materials, 322 (4), 427-433.

**6.** Phan, M.H., Tian, S.B., Hoang, D.Q., Yu, S.C., Nguyen, C., Ulyanov, A.N., 2003. Large Magnetic-entropy Change Above 300K in CMR Materials. Journal of Magnetism and Magnetic Materials, 258-259 (Supplement C), 309-311.

**7.** Rebello, A., Naik, V.B., Mahendiran, R., 2011. Large Reversible Magnetocaloric Effect in $La_{0.7-x}Pr_xCa_{0.3}MnO_3$. Journal of Applied Physics, 110 (1), 013906.

**8.** Wang, Z., Xu, Q., Ni, G., Zhang, H., 2011. Magnetic Entropy Change in Perovskite Manganites $La_{0.6}Pr_{0.1}Pb_{0.3}MnO_3$ With Double Metal–insulator Peaks. Physica B: Condensed Matter, 406 (23), 4333-4337.

**9.** Zhong, W., Chen, W., Au, C.T., Du, Y.W., 2003. Dependence of the Magnetocaloric Effect on Oxygen Stoichiometry in Polycrystalline $La_{2/3}Ba_{1/3}MnO_{3-\delta}$. Journal of Magnetism and Magnetic Materials, 261 (1), 238-243.

**10.** Reis, M.S., Amaral, V.S., Araújo, J.P., Tavares, P.B., Gomes, A.M., Oliveira, I.S., 2005. Magnetic Entropy Change of $Pr_{1-x}Ca_xMnO_3$ Manganites ($0.2<x<0.95$). Physica Review B, 71 (14), 144413.

**11.** Bejar, M., Dhahri, E., Hlil, E.K., Heniti, S., 2007. Influence of A-site Cation Size-disorder on Structural, Magnetic and Magnetocaloric Properties of $La_{0.7}Ca_{0.3-x}K_xMnO_3$ Compounds. Journal of Alloys and Compounds, 440 (1), 36-42.

**12.** Aliev, A.M., Gamzatov, A.G., Batdalov, A.B., Mankevich, A.S., Korsakov, I.E., 2011. Structure and Magnetocaloric Properties of $La_{1-x}K_xMnO_3$ Manganites. Physica B: Condensed Matter, 406 (4), 885-889.

**13.** Dayal, V., Punith Kumar, V., 2014. Investigation of Complex Magnetic State in $La_{0.8}Bi_{0.2}MnO_3$. Journal of Magnetism and Magnetic Materials, 361 (Supplement C), 212-218.

**14.** Ayaş, A.O., Akyol, M., Ekicibil, A., 2016. Structural and Magnetic Properties with Large Reversible Magnetocaloric Effect in $(La_{1-x}Pr_x)_{0.85}Ag_{0.15}MnO_3$ $(0.0\leq x\leq 0.5)$ Compounds. Philosophical Magazine, 96 (10), 922-937.

**15.** Ayas, A.O., 2017. $(La_{0.9}Gd_{0.1})_{0.85}Ag_{0.15}MnO_3$ Manyetik Soğutucu Malzemede Kısmi Gd Değişiminin Yapısal, Manyetik ve Manyetik Soğutma Özellikleri Üzerine Etkisi. Fırat Üniversitesi Mühendislik Bilimleri Dergisi, 29 (2), 155-162.

**16.** Tang, T., Gu, K.M., Cao, Q.Q., Wang, D.H., Zhang, S.Y., Du, Y.W., 2000. Magnetocaloric Properties of Ag-substituted Perovskite-type Manganites. Journal of Magnetism and Magnetic Materials 222 (1), 110-114.

**17.** Kamilov, I.K., Gamzatov, A.G., Aliev, A.M., Batdalov, A.B., Aliverdiev, A.A., Sh, B.A., 2007. Magnetocaloric Effect in $La_{1-x}Ag_y$ $MnO_3$ $(y\leq x)$: Direct and İndirect Measurements. Journal of Physica D: Applied Physics, 40 (15), 4413.

**18.** Muñoz, A., Alonso, J.A., Martínez-Lope, M.J., Pomjakushin, V., André, G., 2012. On the Magnetic Structure of $PrMn_2O_5$: a Neutron Diffraction Study. Journal of Physics: Condensed Matter, 24 (7), 076003.

**19.** Shannon, R.D., 1976. Revised Effective Ionic Radii and Systematic Studies of Interatomic Distances in Halides and Chalcogenides. Acta Crystallographica Section A, 32 (5), 751-767.

**20.** Koubaa, M., Cheikh-Rouhou Koubaa, W., Cheikhrouhou, A., 2009. Magnetocaloric Effect in Polycrystalline $La_{0.65}Ba_{0.3}M_{0.05}MnO_3$ (M=Na, Ag, K) Manganites. Journal of Magnetism and Magnetic Materials, 321(21), 3578-3584.

**21.** M'nassri, R., Cheikhrouhou-Koubaa, W., Koubaa, M., Boudjada, N., Cheikhrouhou, A., 2011. Magnetic and Magnetocaloric Properties of $Pr_{0.6-x}Eu_xSr_{0.4}MnO_3$ Manganese Oxides. Solid State Communications, 151(21), 1579-1582.

**22.** Chen, W., Zhong, W., Hou, D.L., Gao, R.W., Feng, W.C., Zhu, M.G., 2002. Preparation and Magnetocaloric Effect of Self-doped $La_{0.8-x}Na_{0.2x}MnO_{3+\delta}$ Polycrystal. Journal of Physics: Condensed Matter, 14(45), 11889.

**23.** Morrish, A.H., 1965. The Physical Principles of Magnetism. New York: Wiley.

**24.** Dudric, R., Goga, F., Mican, S., Tetean, R., 2013. Effects of Substitution of Pr, Nd, and Sm for La on the Magnetic Properties and Magnetocaloric Effect of $La_{1.4}Ca_{1.6}Mn_2O_7$. Journal of Alloys and Compounds, 553 (Supplement C), 129-134.

**25.** Phan, T.L., Ho, T.A., Thang, P.D., Tran, Q.T., Thanh, T.D., Phuc, N.X., 2014. Critical Behavior of Y-doped $Nd_{0.7}Sr_{0.3}MnO_3$ Manganites Exhibiting the Tricritical Point and Large Magnetocaloric Effect. Journal of Alloys and Compounds, 615(Supplement C), 937-945.